IEEE Access
Multidisciplinary | Rapid Review | Open Access Journal

Received 2 June 2024, accepted 6 July 2024, date of publication 9 July 2024, date of current version 17 July 2024.

Digital Object Identifier 10.1109/ACCESS.2024.3425667

RESEARCH ARTICLE

Zero Dynamic Active Suppression Control for Underactuated Reusable Launch Vehicles With Nonminimum Phase Property

YUXIAO WANG, YUYU ZHAO, AND GAOWEI ZHANG
College of Electronic Information and Automation, Civil Aviation University of China, Tianjin 300300, China

Corresponding author: Yuyu Zhao (yy_zhao@cauc.edu.cn)

This work was supported in part by the National Natural Science Foundation of China under Grant 62003351 and Grant 62003352; in part by the Fundamental Research Funds for the Central Universities (CAUC) under Grant 3122019055, Grant 3122019053, and Grant 3122023QD06; and in part by the Research Start-Up Fund (CAUC) under Grant 2020KYQD11.

ABSTRACT This paper investigates the attitude controller design for an underactuated reusable launch vehicle (RLV) with nonminimum phase property. To address the nonminimum phase problem, a zero dynamic active suppression control (ZDASC) method based on Byrnes-Isidori (B-I) standard model transformation is proposed. First, a computable criterion for the nonminimum phase property of RLVs is presented, by which we can effectively determine the nonminimum phase property based on aerodynamic parameters in the RLV model. Second, an augmented system consisting of internal dynamics and dynamic compensator is constructed, and a ZDASC method is proposed for the RLV attitude control system with nonminimum phase property, which can enable adaptive stabilization of the RLV's zero dynamics under different operating conditions and uncertainties. ZDASC achieves output accurate tracking without solving the ideal internal dynamics, which reduces the computational complexity and enhances system robustness. Finally, simulation results of the RLV attitude control are provided to verify the effectiveness and robustness of the proposed controller in tracking the guidance commands as well as stabilizing the internal dynamics.

INDEX TERMS Zero dynamic active suppression, attitude control, underactuated, nonminimum phase, reusable launch vehicle.

I. INTRODUCTION

In the last decades, reusable launch vehicles (RLVs) received much more attention due to their great potential to provide an economic way to enter space in the future [1], [2]. RLVs can achieve low-cost space accesses by recovering and reusing after each mission [3], [4]. However, in the reentry phase, the RLV dynamics are highly nonlinear, multi-variable and uncertain, due to the extreme atmospheric conditions which may include aerodynamic disturbances, heating and gravitational pull. Hence, designing a robust and reliable reentry attitude controller for RLV is necessary to guarantee an accurate orientation against various uncertainties [5].

Some traditional methods are widely used in attitude control of RLVs. In [6] and [7], PID controllers combined with model linearization have been designed, demonstrating good control performance under nominal flight conditions. In [8], a linear quadratic regulator (LQR) controller is designed, which ensures optimality in the digital autopilot (DAP) design of the integrated system. Other linear control methods have also achieved valuable results, such as gain scheduling [9], H_∞ control [10], etc. Nevertheless, linear-based control methods have an undeniable drawback, which is that their control stability can only be maintained at some specific equilibrium points. In practice, the controllers need to face systems with high nonlinearity under large operating ranges, and the performance of linear control methods would be degraded even be unstable. Thus, many nonlinear control methods are developed to improve the performance of RLV's attitude control, such as dynamic inversion control [11], back-stepping control [3], [12], [13], state-dependent Riccati equation [14], and Theta-D control [15]. In particular,

The associate editor coordinating the review of this manuscript and approving it for publication was Xiwang Dong.

sliding mode control (SMC) has the significant advantage of dealing with the model uncertainty and external disturbance [16], [21]. In [16], a novel quaternion observer-based sliding mode attitude fault tolerant scheme is proposed to guarantee the closed-loop system stability and high-precise attitude tracking of RLVs during the reentry stage. In [17], a novel continuous attitude control algorithm is developed utilizing the techniques of super-twisting and terminal sliding mode control synthetically. In [18], a global terminal sliding mode controller based on the quick reaching law is designed, which is proved to converge to the sliding mode surface in a finite time. In [19], a disturbance sliding mode observer is designed, whose output is used as the feed forward compensation for the system speed. In [20], a novel robust controller combining SMC and a nonlinear disturbance observer is designed, which can enhance the longitudinal manoeuvrability of a morphing aircraft. In [21], a control methodology based on an extended state observer (ESO) and SMC is designed for powered parafoil systems, which can effectively overcome the influence of environmental disturbances and achieve accurate trajectory tracking control. It is worth noting that all the aforementioned methods are based on the assumption that the aerodynamic control surfaces of RLVs can provide moments about all three body axes, neglecting the fact that RLVs may experience limited control authority.

In the reentry phase, RLVs may face severe aerodynamic heating due to the large flight dynamic pressure. Furthermore, when the fuselage blocks the airflow around the rudder at a high angle of attack, the rudder's efficiency decreases seriously. Generally, the rudders of RLVs will not be available until the Mach number is less than 6 [22]. During this period, RLV attitude control system is an underactuated system, whose three attitude outputs are controlled by only two body flaps. What's even more tricky is that an underactuated RLV exhibits nonminimum phase behavior [23], [24], which means the system has unstable zero dynamics. Many traditional methods, such as backstepping, dynamic inversion, cannot be directly applied due to the existence of unstable zero dynamics. Therefore, the nonminimum phase property must be addressed to achieve stable attitude control of RLVs. To date, the researches on underactuated nonminimum phase RLVs are not plentiful. Among the results given in the literatures, the representative ideas mainly include output redefinition [24], [25], [26] and dynamic sliding mode control (DSMC) [23], [27], [28]. Tian and Ye have achieved beneficial results by output redefinition in the study of nonminimum phase RLVs control [25], [26]. In [25], they incorporated ideal internal dynamics(IIDs) into RLV attitude control method for the first time, which greatly improves the output tracking accuracy for time-varying signals. Furthermore, they considered the input constraint, and proposed an anti-windup strategy by using feedback error clipping. It is shown that the input saturation can be effectively avoided [26]. IIDs can be calculated by several methods, such as output regulation [29], [30], stable system center [31], [32], stable inversion [33], [34], and optimal bounded inversion. Nevertheless, the calculation of IID relies on accurate models, which may bring additional uncertainty to the system. In [23], a second-order sliding mode control method is proposed to stabilize the unstable internal dynamics of the system. The disadvantage of this method is that it is only effective for systems with a relative order of 2, and the setting of the sliding mode surface will imprison the equilibrium points of the internal dynamics, resulting in a loss of tracking performance in the presence of uncertainty [35].

In this article, a zero dynamic active suppression control (ZDASC) method is proposed to realize the stable attitude control for underactuated nonminimum RLVs. First, the RLV attitude model is transformed into a B-I standard model, which realize the decoupling between internal dynamics and control inputs. Then, a computable criterion for the nonminimum phase property of RLVs is presented, by which we can effectively determine the nonminimum phase property based on aerodynamic parameters in the RLV model. Second, a ZDASC method is proposed, transforming an attitude output tracking task into a stabilization task of an augmented system consisting of internal dynamics and a dynamic compensator. ZDASC can achieve output accurate tracking without solving the ideal internal dynamics, which reduces the computational complexity and enhances system robustness. In particular, the overall approach shown here provides a practical solution to achieving RLV reentry attitude tracking control under realistic conditions. Compared with the existing methods [23], [27], the proposed method can greatly improve the output tracking accuracy and smooth the process status and control inputs. Then, it confirms the robustness of the proposed method by Monte Carlo simulations in this work. The main contributions of this study are summarized as follows.

a) A nonminimum phase criterion based on the B-I standard model is presented, revealing the mathematical essence of nonminimum phase behavior. On the basis of this criterion, we can determine whether RLV has non minimum phase behavior by its model parameters, and this criterion also has reference significance for the determination of other nonminimum phase systems.

b) ZDASC method takes into account the stabilization of the internal dynamics of the system in the natural control channel. It achieves output accurate tracking without solving the ideal internal dynamics, which reduces the computational complexity and enhances system robustness.

c) Compared to the second-order dynamic sliding mode control (SODSMC) method in [23], ZDASC does not fix its convergence origin when stabilizing the internal dynamics of the system, thus achieving internal dynamic adaptive balance under different operating conditions and uncertainties. The proposed ZDASC method has better tracking performance and stronger robustness.

The remainder of this article is organized as follows. Section II introduces the underactuated nonminimum RLV model. In Section III, the zero dynamics are analyzed base on B-I standard model transformation, and a computable criterion for the nonminimum phase property of RLVs is presented. In Section IV, a ZDASC method is proposed to realize the outputs accuracy tracking and zero dynamics stabilization. Numerical simulation results are given in Section V and conclusions are given in Section 6.

II. PROBLEM FORMULATION

In this section, the attitude dynamics model is established for an underactuated RLV with two body flaps. The rear view of the vehicle is shown in Fig. 1. Differential deflection of body flaps achieves aileron operation, and body flaps rotated in the same direction achieves elevator operation.

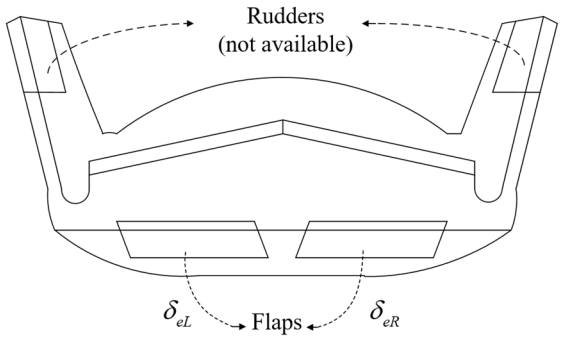

FIGURE 1. The rear view of the vehicle.

A. ATTITUDE CONTROL MODEL

Assuming zero flight path angle based on the quasi equilibrium glide condition, the RLV rigid-body attitude dynamics [23] are given in (1).

$$\begin{cases} \dot{\alpha} = -p\cos\alpha\tan\beta + q - r\sin\alpha\tan\beta \\ \qquad + \dfrac{m_0 g_0\cos\mu - L}{m_0 V_0\cos\beta} \\ \dot{\beta} = p\sin\alpha - r\cos\alpha + \dfrac{m_0 g_0\sin\mu - Y}{m_0 V_0} \\ \dot{\mu} = \dfrac{p\cos\alpha + r\sin\alpha}{\cos\beta} + \dfrac{L - m_0 g_0\cos\mu}{m_0 V_0}\tan\beta \\ \dot{p} = \dfrac{I_{xz}\left(I_x - I_y + I_z\right)pq + \left(I_y I_z - I_z^2 - I_{xz}^2\right)qr}{I_x I_z - I_{xz}^2} \\ \qquad + L'_\beta\beta + L'_{\delta_a}\delta_a \\ \dot{q} = \dfrac{\left(I_z - I_x\right)pr + I_{xz}\left(r^2 - p^2\right)}{I_y} + M'_\alpha\Delta\alpha + M'_{\delta_e}\Delta\delta_e \\ \dot{r} = \dfrac{I_{xz}\left(-I_x + I_y - I_z\right)qr + \left(I_x^2 - I_x I_y + I_{xz}^2\right)pq}{I_x I_z - I_{xz}^2} \\ \qquad + N'_\beta\beta + N'_{\delta_a}\delta_a \end{cases} \tag{1}$$

where α, β, and μ are the angle of attack, sideslip angle, and bank angle, respectively. p, q, and r are roll rate, pitch rate, and yaw rate, respectively. I_x, I_y,and I_z are the moments of inertia about x-, y-, and z-body axes, and I_{xz} denotes the cross product of inertia with respect to x- and z-body axes. m_0, V_0 and g_0 denote the vehicle mass, flight pass velocity, and gravitational acceleration, respectively. $L = L_a\Delta\alpha + m_0 g_0$ denotes the lift, $Y = Y_\beta\beta$ denotes the side force, respectively. L_a, Y_β, L'_β, L'_{δ_a}, N'_β, N'_{δ_a}, M'_α and M'_{δ_e} are aerodynamic parameters. The complete aerodynamic parameters are given in [36]. The $\Delta\alpha = \alpha - \alpha_T$, $\Delta\delta_e = \delta_e - \delta_{eT}$ denote deviations of α and δ_e from trim condition of the flight dynamics, where α_T and δ_{eT} denote the trim angle of attack and the trim elevator deflection, respectively. Usually α_T is a prescribed function of the Mach number. Because the evolution of the Mach number is slower than the attitude dynamics, α_T is taken as constant. δ_{eT} corresponds to the trim elevator when the pitching moment of the vehicle is free. Also, the changes in m_0, V_0, and g_0 are considered slower than the changes in attitude states [24], so they are considered constants in attitude control systems. In general, control surfaces are primarily moment-producing devices, their influences on lift and side force are much smaller than the influences of airflow angles. Thus, the influence of the control effectors on lift and side force will be ignored. This approach has been verified viable by many flight control applications [37].

B. B-I NORMALIZED TRANSFORMATION

A new evaluation criterion is proposed for the nonminimum phase property of the vehicle in this section. Without any loss of generality, the affine nonlinear control system is described as

$$\begin{aligned} \dot{\boldsymbol{x}} &= \boldsymbol{f}(\boldsymbol{x}) + \boldsymbol{g}(\boldsymbol{x})\boldsymbol{u} \\ \boldsymbol{y} &= \boldsymbol{h}(\boldsymbol{x}) \end{aligned} \tag{2}$$

where

$$\begin{aligned} \boldsymbol{x} &= [x_1, x_2, \cdots, x_n]^{\mathrm{T}} \\ \boldsymbol{u} &= [u_1, u_2, \cdots, u_m]^{\mathrm{T}} \\ \boldsymbol{y} &= [y_1, y_2, \cdots, y_m]^{\mathrm{T}} \\ \boldsymbol{f}(\boldsymbol{x}) &= [f_1(\boldsymbol{x}), f_2(\boldsymbol{x}), \cdots, f_n(\boldsymbol{x})]^{\mathrm{T}} \\ \boldsymbol{h}(\boldsymbol{x}) &= [h_1(\boldsymbol{x}), h_2(\boldsymbol{x}), \cdots, h_m(\boldsymbol{x})]^{\mathrm{T}} \\ \boldsymbol{g}(\boldsymbol{x}) &= \begin{bmatrix} g_1(\boldsymbol{x}) & \cdots & g_{1m}(\boldsymbol{x}) \\ \vdots & \ddots & \vdots \\ g_{n1}(\boldsymbol{x}) & \cdots & g_{nm}(\boldsymbol{x}) \end{bmatrix}^{\mathrm{T}} \end{aligned} \tag{3}$$

Here, we assume that the system has a vector relative degree $[\rho_1, \rho_2, \cdots, \rho_m]^{\mathrm{T}}$. Since the relative degree ρ of affine system (2) is less than the number of states n, the system inevitably exists internal dynamics. In order to study the internal dynamics of the system more conveniently, it is hoped that the nonminimum phase system can be transformed into B-I normalized form by a coordinate transformation:

$$\Phi(\boldsymbol{x}) : \boldsymbol{x} \to (\boldsymbol{\xi}, \boldsymbol{\eta}) \tag{4}$$

where $\boldsymbol{x} \in \mathbb{R}^n$ is the state vector of an n-th order system. $\boldsymbol{\xi}$ and $\boldsymbol{\eta}$ denote external states and internal states, respectively. The

transformation can achieve decoupling of internal dynamics from control input $\boldsymbol{u}$.

The m dynamic equations of the B-I normalized form that depend explicitly on the control variables can be put in the following form:

$$\dot{\boldsymbol{\xi}}_\rho = \boldsymbol{b}(\boldsymbol{\xi}, \boldsymbol{\eta}) + \boldsymbol{a}(\boldsymbol{\xi}, \boldsymbol{\eta})\boldsymbol{u} \tag{5}$$

where $\boldsymbol{\xi}_\rho \in \mathbb{R}^m$, $\forall \boldsymbol{\xi}_\rho \in \left[\begin{array}{ccc} \xi_{\rho_1}^1 & \cdots & \xi_{\rho_m}^m \end{array}\right]^{\mathrm{T}}$.

If the matrix $\boldsymbol{a}(\boldsymbol{\xi}, \boldsymbol{\eta})$ is locally nonsingular, the rigorous input–output feedback linearization is obtained as follows:

$$\boldsymbol{u} = \boldsymbol{a}^{-1}(\boldsymbol{\xi}, \boldsymbol{\eta})(-\boldsymbol{b}(\boldsymbol{\xi}, \boldsymbol{\eta}) + \boldsymbol{v}) \tag{6}$$

Substitution of (6) into B-I normalized form (2) yields

$$\begin{cases} \dot{\xi}_j^i = \xi_{j+1}^i \\ \dot{\xi}_\rho^i = v_i \\ \dot{\boldsymbol{\eta}} = \boldsymbol{q}(\boldsymbol{\xi}, \boldsymbol{\eta}) \end{cases} \tag{7}$$

where $\boldsymbol{\eta}$ is the internal dynamics and v_i is the pseudo control input of the i-th control channel.

C. NONMINIMUM PHASE OF RLVS

There exists a similar coordinate transformation such that the underactuated hypersonic vehicle model (1) could be converted into a normal form like (7).

The control goal of the RLV attitude dynamics model (1) is to track the angle of attack profile and the bank angle profile given in real time, and to keep the sideslip angle near zero at the same time. Consider the angle of attack α and the bank angle μ as the model outputs, and $\boldsymbol{u} = \left[\begin{array}{cc} \delta_e & \delta_a \end{array}\right]^{\mathrm{T}}$ is the control input vector. Then the model (1) has a vector relative degree $\left[\begin{array}{cc} \rho_1 & \rho_2 \end{array}\right] = \left[\begin{array}{cc} 2 & 2 \end{array}\right]$, and that $\rho = 4 < n = 6$, the system inevitably exists 2-order internal dynamics. According to model (1) and the 2 outputs α and μ, the natural external state vector is represented as

$$\begin{aligned} \boldsymbol{\xi} &= \left[\begin{array}{cc} \boldsymbol{\xi}_1 & \boldsymbol{\xi}_2 \end{array}\right]^{\mathrm{T}} \\ &= \left[\begin{array}{cccc} \xi_{11} & \xi_{12} & \xi_{21} & \xi_{22} \end{array}\right]^{\mathrm{T}} \\ &= \left[\begin{array}{cccc} \Delta\alpha & q & \mu & p \end{array}\right]^{\mathrm{T}} \end{aligned} \tag{8}$$

In order to remove the control inputs in the internal dynamics, the 2-order internal states are represented as follows:

$$\begin{aligned} \boldsymbol{\eta} &= \left[\begin{array}{cc} \eta_1 & \eta_2 \end{array}\right]^{\mathrm{T}} \\ &= \left[\begin{array}{cc} \beta & \frac{p}{L'_{\delta_a}} - \frac{r}{N'_{\delta_a}} \end{array}\right]^{\mathrm{T}} \end{aligned} \tag{9}$$

Theorem 1: If the RLV system trim states and parameters satisfy (10), the RLV attitude control system is a nonminimum phase system.

$$\cos\alpha_T N'_{\delta_e}\left(\frac{L'_\beta}{L'_{\delta_a}} - \frac{N'_\beta}{N'_{\delta_a}}\right) > 0 \tag{10}$$

Proof: The stability of the zero dynamics is analyzed under the trim condition to evaluate the stability of the internal dynamics. We assume that $\alpha = \alpha_T$, $\gamma_0 \approx 0$, $p = q = 0$, and the zero dynamics

$$\left[\begin{array}{c} \dot{\eta}_1 \\ \dot{\eta}_2 \end{array}\right] = \left[\begin{array}{cc} \frac{-Y_\beta}{m_0 V_0} & \cos\alpha_T N'_{\delta_e} \\ \frac{L'_\beta}{L'_{\delta_a}} - \frac{N'_\beta}{N'_{\delta_a}} & 0 \end{array}\right] \left[\begin{array}{c} \eta_1 \\ \eta_2 \end{array}\right] \tag{11}$$

The eigenvalue vector of the state matrix of (11) is the dominant factor affecting the stability of the zero dynamics. It can be calculated as

$$\lambda^2 + \frac{Y_\beta}{m_0 V_0}\lambda - \cos\alpha_T N'_{\delta_e}\left(\frac{L'_\beta}{L'_{\delta_a}} - \frac{N'_\beta}{N'_{\delta_a}}\right) = 0 \tag{12}$$

If inequality (10) holds, there exist at least one positive eigenvalue. The zero dynamics (11) is unstable, and the RLV attitude control system is a nonminimum phase system. □

The theorem 1 provides an aerodynamic-parameter-depended nonminimum phase criterion for the analysis of RLV attitude control system.

III. ZERO DUNAMIC ACTIVE SUPPRESSION ATTITUDE CONTROL FOR RLVS

In this section, a zero dynamic active suppression attitude control method is proposed for underactuated nonminimum attitude system of RLV. From (1), we can see that the longitudinal control channel is almost naturally decoupled, as the sideslip angle $\beta \approx 0$ throughout the control process. In addition, the internal dynamics $\left[\begin{array}{cc} \dot{\eta}_1 & \dot{\eta}_2 \end{array}\right]^{\mathrm{T}}$ are linearly dependent on lateral states $\left[\begin{array}{cccc} \beta & \mu & p & r \end{array}\right]^{\mathrm{T}}$, and linearly independent on vertical states $\left[\begin{array}{cc} \alpha & q \end{array}\right]^{\mathrm{T}}$. Thus, the system can be decomposed into the following two subsystems: the minimum phase longitudinal control subsystem and the nonminimum phase lateral control subsystem. This segmentation method is common and acceptable [23], which is beneficial to the ZDASC design.

A. CONTROLLER DESIGN FOR LONGITUDINAL DYNAMICS OF MINIMUM PHASE

The longitudinal model is described as

$$\begin{cases} \dot{\alpha} = q + w_{11} \\ \dot{q} = w_{12} + b_1 \Delta\delta_e \end{cases} \tag{13}$$

where $\boldsymbol{w}_1 = \left[\begin{array}{cc} w_{11} & w_{12} \end{array}\right]^{\mathrm{T}}$ is the nonlinear term vector of $\dot{\alpha}$ and $\dot{q}$ in (1), and $b_1 = M'_{\delta_e}$

Let $\boldsymbol{\xi}_1 = \left[\begin{array}{cc} \xi_{11} & \xi_{12} \end{array}\right]^{\mathrm{T}} = \left[\begin{array}{cc} \alpha & \dot{\alpha} \end{array}\right]^{\mathrm{T}}$, and a dynamic inverse control law (14) is designed to achieve model linearization.

$$\Delta\delta_e = \frac{1}{b_1}(v_1 - w_{12} - \dot{w}_{11}) \tag{14}$$

then model (13) becomes

$$\begin{cases} \dot{\xi}_{11} = \xi_{12} \\ \dot{\xi}_{12} = v_1 + d_1 \end{cases} \tag{15}$$

where v_1 is a virtual control variable, and d_1 represents the modeling errors and unknown disturbance uncertainty in the longitudinal dynamics, with the assumption that d_1 is bounded within certain limits.

Lemma 1 [38]: Suppose there exists a continuous differential positive-definite function $V(\boldsymbol{x}): D \to R$, real numbers $p > 0, 0 < \eta < 1$,such that

$$\dot{V}(\boldsymbol{x}) + pV^{\eta}(\boldsymbol{x}) \leq 0, \quad \forall \boldsymbol{x} \in D \tag{16}$$

Then, the origin of system $\dot{\boldsymbol{x}} = \boldsymbol{f}(\boldsymbol{x})$ is a locally finite-time stable equilibrium, and the settling time, depending on the initial state $\boldsymbol{x}_0$, satisfies

$$T(\boldsymbol{x}_0) \leq \frac{V^{1-\eta}(\boldsymbol{x}_0)}{p(1-\eta)} \tag{17}$$

The sliding surface for longitudinal control is represented as

$$S_1 = c_1 e_1 + e_2 \tag{18}$$

where $e_1 = \xi_{11} - \xi_{11c}$, $e_2 = \xi_{12} - \xi_{12c}$, and c_1 is a positive constant parameter.

The conventional sliding mode control (SMC) law is

$$v_1 = -\lambda_{11}\mathrm{sgn}(S_1) - \lambda_{12}\mathrm{sgn}(S_1)|S_1|^{\alpha_1} - c_1\dot{e}_1 + \dot{\xi}_{12c} \tag{19}$$

where $\lambda_{11} > \sup_{t>0}\|d_1(t)\|$, $-1 < \alpha_1 < 1$. Choosing the candidate of Lyapunov function as $V_1 = \frac{1}{2}S_1^2$, the derivative of V_1

is given by

$$\begin{aligned}\dot{V}_1 &= S_1\dot{S}_1 = S_1\left(c_1\dot{e}_1 + \dot{\xi}_{12} - \dot{\xi}_{12c}\right)\\ &= S_1\begin{pmatrix} c_1\dot{e}_1 - \lambda_1\mathrm{sign}(S_1) - \lambda_{12}\mathrm{sgn}(S_1)|S_1|^{\alpha_1} \\ -c_1\dot{e}_1 + \dot{\xi}_{12c} + d_1 - \dot{\xi}_{12c}\end{pmatrix}\\ &= \left(-\lambda_1\mathrm{sgn}(S_1) + d_1 - \lambda_{12}\mathrm{sgn}(S_1)|S_1|^{\alpha_1}\right)S_1\\ &< -\lambda_{12}\mathrm{sgn}(S_1)|S_1|^{\alpha_1}S_1\end{aligned} \tag{20}$$

Using $\mathrm{sgn}(S_1) = \frac{|S_1|}{S_1}$, we have

$$\begin{aligned}\dot{V}_1 &< -\lambda_{12}|S_1|^{\alpha_1+1}\\ &= -2^{\frac{\alpha_1+1}{2}}\lambda_{12}\left(\frac{1}{2}S_1^2\right)^{\frac{\alpha_1+1}{2}}\\ &= -2^{\frac{\alpha_1+1}{2}}\lambda_{12}V_1^{\frac{\alpha_1+1}{2}}\end{aligned} \tag{21}$$

According to Lemma 1, the state trajectories will reach toward the sliding surface $S_1 = 0$ in finite time and remain sliding on it. We get

$$e_2 = -c_1 e_1 \tag{22}$$

Obviously, after a sufficient amount of time, the tracking errors e_1 and e_2 will converge to origin simultaneously.

B. CONTROLLER DESIGN FOR LATERAL DYNAMICS OF NONMINIMUM PHASE

The lateral model is described as

$$\begin{cases}\dot{\beta} = p\sin\alpha - r\cos\alpha + \dfrac{m_0 g_0\sin\mu\cos\gamma_0 - Y}{m_0 V_0}\\ \dot{\mu} = \dfrac{p\cos\alpha + r\sin\alpha}{\cos\beta} + \dfrac{L - m_0 g_0\cos\mu\tan\gamma_0}{m_0 V_0}\tan\beta\\ \qquad + \dfrac{\tan\gamma_0}{m_0 V_0}(Y\cos\mu + L\sin\mu)\\ \dot{p} = \dfrac{I_{xz}\left(I_x - I_y + I_z\right)pq + \left(I_y I_z - I_z^2 - I_{xz}^2\right)qr}{I_x I_z - I_{xz}^2}\\ \qquad + L'_\beta\beta + L'_{\delta_a}\delta_a\\ \dot{r} = \dfrac{I_{xz}\left(-I_x + I_y - I_z\right)qr + \left(I_x^2 - I_x I_y + I_{xz}^2\right)pq}{I_x I_z - I_{xz}^2}\\ \qquad + N'_\beta\beta + N'_{\delta_a}\delta_a\end{cases} \tag{23}$$

The SMC in Section III-A is used with limits for the nonminimum phase lateral subsystem, due to the unstable zero dynamics (11). An alternative control scheme needs to be designed to stabilize the zero dynamics of the system.

Let $\boldsymbol{\xi}_2 = \begin{bmatrix}\xi_{21} & \xi_{22}\end{bmatrix}^{\mathrm{T}} = \begin{bmatrix}\mu - \mu_c & p\end{bmatrix}^{\mathrm{T}}$, and $\boldsymbol{\eta} = \begin{bmatrix}\eta_1 & \eta_2\end{bmatrix}^{\mathrm{T}} = \begin{bmatrix}\beta & \frac{p}{L'_{\delta_a}} - \frac{r}{N'_{\delta_a}}\end{bmatrix}^{\mathrm{T}}$, and a dynamic inverse control law (24) is designed to achieve model linearization.

$$\delta_a = \frac{1}{L'_{\delta_a}}\begin{pmatrix} v_2 - \dfrac{I_{xz}\left(I_x - I_y + I_z\right)pq}{I_x I_z - I_{xz}^2} \\ -\dfrac{\left(I_y I_z - I_z^2 - I_{xz}^2\right)qr}{I_x I_z - I_{xz}^2} - L'_\beta\beta\end{pmatrix} \tag{24}$$

then model (23) becomes

$$\begin{cases}\dot{\xi}_{21} = \boldsymbol{A}_{\xi_2}\boldsymbol{\xi}_2 + \boldsymbol{A}_\eta\,\boldsymbol{\eta} - \dot{\mu}_c\\ \dot{\xi}_{22} = v_2 + d_2\\ \dot{\boldsymbol{\eta}} = \boldsymbol{B}_{\xi_2}\boldsymbol{\xi}_2 + \boldsymbol{B}_\eta\boldsymbol{\eta}\end{cases} \tag{25}$$

where

$$\boldsymbol{A}_{\xi_2} = \begin{bmatrix}0 & \dfrac{\cos\alpha}{\cos\beta} + \dfrac{\sin\alpha N'_{\delta_a}}{\cos\beta L'_{\delta_a}}\end{bmatrix} \tag{26}$$

$$\boldsymbol{A}_\eta = \begin{bmatrix}\dfrac{\begin{pmatrix}L - mg_0\cos\mu \\ +Y_\beta\tan V_0\cos\mu\end{pmatrix}}{mV_0} & -\dfrac{\sin\alpha N'_{\delta_a}}{\cos\beta}\end{bmatrix} \tag{27}$$

$$\boldsymbol{A}_u = \begin{bmatrix}0\\1\end{bmatrix} \tag{28}$$

$$\boldsymbol{B}_{\xi_2} = \begin{bmatrix}\dfrac{g_0}{V_0} & \sin\alpha - \dfrac{\cos\alpha N'_{\delta_a}}{L'_{\delta_a}}\\ 0 & q\begin{bmatrix}\dfrac{2I_{xz}\left(I_x - I_y + I_z\right)}{\left(I_x I_z - I_{xz}^2\right)L'_{\delta_a}}\\ -\dfrac{\left(I_x^2 - I_x I_y + I_{xz}^2\right)}{\left(I_x I_z - I_{xz}^2\right)N'_{\delta_a}}\\ +\dfrac{N'_{\delta_a}\left(I_y I_z - I_z^2 - I_{xz}^2\right)}{\left(I_x I_z - I_{xz}^2\right)L'^2_{\delta_a}}\end{bmatrix}\end{bmatrix} \tag{29}$$

$$\boldsymbol{B}_\eta = \begin{bmatrix} \dfrac{-Y_\beta}{m_0 V_0} & \cos\alpha N'_{\delta_a} \\ \dfrac{L'_\beta}{L'_{\delta_a}} - \dfrac{N'_\beta}{N'_{\delta_a}} & \dfrac{q\begin{bmatrix} N'_{\delta_a}\left(I_y I_z - I_z^2 - I_{xz}^2\right) \\ -L'_{\delta_a} I_{xz}\left(-I_x + I_y - I_z\right)\end{bmatrix}}{-\left(I_x I_z - I_{xz}^2\right) L'_{\delta_a}} \end{bmatrix} \tag{30}$$

In (25), v_2 is a virtual control variable, and d_2 represents the modeling errors and unknown disturbance uncertainty in the lateral dynamics, with the assumption that d_2 is bounded within certain limits.

The matrix $\boldsymbol{B}_\eta$ is non-Hurwitz because of the nonminimum nature of the system. As time increase, the zero dynamics will diverge uncontrollably as (31).

$$\lim_{t\to\infty} \left\| \begin{matrix} \eta_1 \\ \eta_2 \end{matrix} \right\| = \infty \tag{31}$$

A ZDASC method is proposed to stabilize the zero dynamics while maintaining precise tracking of expected outputs. In order to achieve active suppression of system zero dynamics, control law design needs to take into account internal dynamics $\dot{\boldsymbol{\eta}}$, rather than only achieving output tracking in external dynamic control channels.

A special dynamic integral sliding mode surface that encompasses internal dynamics for subsystem (25) is defined as

$$S_2 = \xi_{22} - \int_0^t \boldsymbol{G}^{\mathrm{T}} \boldsymbol{X} d\tau \tag{32}$$

where

$$\boldsymbol{X} = \begin{bmatrix} \boldsymbol{\xi}_2^{\mathrm{T}} & \boldsymbol{\eta}^{\mathrm{T}} & \chi \end{bmatrix}^{\mathrm{T}}, \ \boldsymbol{G} = \begin{bmatrix} g_1 & g_2 & g_3 & g_4 & g_5 \end{bmatrix}^{\mathrm{T}}$$

is a parameter vector to be determined. χ is a dynamic compensator, and its updating law is

$$\dot{\chi} = \boldsymbol{F}^{\mathrm{T}} \boldsymbol{X} \tag{33}$$

where

$$\boldsymbol{F} = \begin{bmatrix} f_1 & f_2 & f_3 & f_4 & f_5 \end{bmatrix}^{\mathrm{T}}.$$

Theorem 2: Construct an integrated matrix as follows:

$$\boldsymbol{Q} = \begin{bmatrix} \boldsymbol{A'}^{\mathrm{T}} & \boldsymbol{G} & \boldsymbol{B'}^{\mathrm{T}} & \boldsymbol{F} \end{bmatrix}^{\mathrm{T}} \tag{34}$$

where $\boldsymbol{A'} = \begin{bmatrix} \boldsymbol{A}_{\xi_2} & \boldsymbol{A}_\eta & 0 \end{bmatrix}$, and $\boldsymbol{B'} = \begin{bmatrix} \boldsymbol{B}_{\xi_2} & \boldsymbol{B}_\eta & \boldsymbol{0}_{2\times 1} \end{bmatrix}$.

Design the parameter vectors $\boldsymbol{G}$ and $\boldsymbol{F}$ that make (35) hold, while ensuring that the matrix $\boldsymbol{Q}$ in (34) is Hurwitz.

$$\begin{cases} f_5 g_2 - f_2 g_5 = 0 \\ f_5 g_4 - f_4 g_5 = 0 \end{cases} \tag{35}$$

Let the virtual control law be provided by

$$v_2 = -\lambda_{21} \mathrm{sgn}\left(S_2\right) - \lambda_{22} \mathrm{sgn}\left(S_2\right) |S_2|^{\alpha_2} + \boldsymbol{G}^{\mathrm{T}} \boldsymbol{X} \tag{36}$$

with $\lambda_{21} > \sup_{t>0} \|d_2(t)\|$, $\lambda_{22} > 0$, $-1 < \alpha_2 < 1$. Then control law (36) will achieve the output precise tracking while stabilizing the internal dynamics.

Proof: By choosing the candidate of Lyapunov function as $V_2 = \frac{1}{2} S_2^2$, the derivative of V_2 is expressed as

$$\begin{aligned} \dot{V}_2 = S_2 \dot{S}_2 &= S_2\left(\dot{\xi}_{22} - \boldsymbol{G}^{\mathrm{T}} \boldsymbol{X}\right) \\ &= S_2\left(v_2 + d_2 - \boldsymbol{G}^{\mathrm{T}} \boldsymbol{X}\right) \\ &= \left(-\lambda_{21} \mathrm{sgn}\left(S_2\right) + d_2 - \lambda_{22} \mathrm{sgn}\left(S_2\right) |S_2|^{\alpha_2}\right) S_2 \\ &< -\lambda_{22} \mathrm{sgn}\left(S_2\right) |S_2|^{\alpha} S_2 \\ &= -2^{\frac{\alpha_2+1}{2}} \lambda_{22} V_2^{\frac{\alpha_2+1}{2}} \end{aligned} \tag{37}$$

According to Lemma 1, the state trajectories will reach the sliding mode surface $S_2 = 0$ in finite time and remain sliding on it. Then the external dynamic can be expressed as

$$\dot{\xi}_{22} = \boldsymbol{G}^{\mathrm{T}} \boldsymbol{X} \tag{38}$$

Combining (25), (33) and (38), we obtain an augmented system as (39) with dynamic compensator χ.

$$\begin{bmatrix} \dot{\xi}_{21} \\ \dot{\xi}_{22} \\ \dot{\boldsymbol{\eta}} \\ \dot{\chi} \end{bmatrix} = \begin{bmatrix} A'^T & G & B'^T & F \end{bmatrix}^T \begin{bmatrix} \xi_{21} \\ \xi_{22} \\ \boldsymbol{\eta} \\ \chi \end{bmatrix} + \begin{bmatrix} -\dot{\mu}_c \\ 0 \\ 0 \\ 0 \end{bmatrix} \tag{39}$$

As the matrix $\boldsymbol{Q} = \begin{bmatrix} \boldsymbol{A'}^{\mathrm{T}} & \boldsymbol{G} & \boldsymbol{B'}^{\mathrm{T}} & \boldsymbol{F} \end{bmatrix}^{\mathrm{T}}$ is Hurwitz, it can be concluded that the system (39) with internal dynamics $\boldsymbol{\eta}$ is bounded-input and bounded-output (BIBO) stable.

The equilibrium point of system (39) is

$$\boldsymbol{x}^* = -\boldsymbol{Q}^{-1} \Gamma \tag{40}$$

where $\boldsymbol{x}^* = \left[\xi_{21}^*, \xi_{22}^*, \eta_1^*, \eta_2^*, \chi^*\right]^{\mathrm{T}}$, $\Gamma = [-\dot{\mu}_c, 0, 0, 0, 0]^{\mathrm{T}}$.

In particular, the equilibrium point of output ξ_{21}^* that we are most concerned with is

$$\xi_{21}^* = \frac{\dot{\mu}_c}{F} \begin{bmatrix} \left(f_5 g_4 - f_4 g_5\right)\left(\sin\alpha - \frac{\cos\alpha N'_{\delta_a}}{L'_{\delta_a}}\right) \\ -\left(f_5 g_2 - f_2 g_5\right)\cos\alpha N'_{\delta_a} \end{bmatrix} \tag{41}$$

where

$$\begin{aligned} F = &\left(\frac{\sin\alpha\cos\alpha N'^2_{\delta_a}}{\cos\beta L'_{\delta_a}} - \frac{\sin^2\alpha N'_{\delta_a}}{\cos\beta} + \frac{\sin\alpha\cos\alpha N'^2_{\delta_a}}{\cos\beta}\right)\left(f_1 g_5 - f_5 g_1\right) \\ &+ \left(\frac{\cos\alpha}{\cos\beta} + \frac{\sin\alpha N'_{\delta_a}}{\cos\beta L'_{\delta_a}}\right)\frac{g_0}{V_0}\left(f_4 g_5 - f_5 g_4\right) \\ &+ \frac{\sin\alpha N'_{\delta_a}}{\cos\beta}\frac{g_0}{V_0}\left(f_2 g_5 - f_5 g_2\right) \end{aligned} \tag{42}$$

It can be seen that ξ_{21}^* is time-varying related to the states of the system and parameters in ZDASC. It is worth noting that when the ZDASC parameters satisfy (35), the equilibrium point of output will be fixed, that is

$$\xi_{21}^* \equiv 0 \tag{43}$$

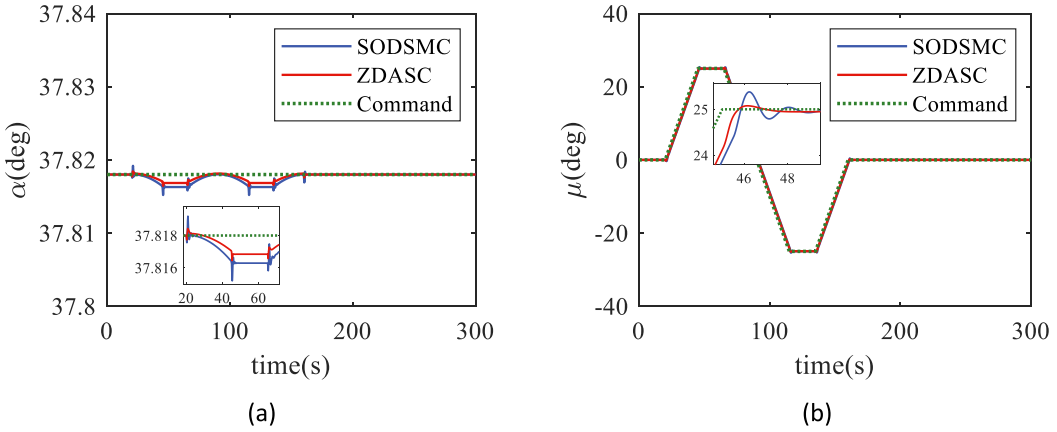

FIGURE 2. Responses of outputs: (a)Angle of attack α, (b) Bank angle μ.

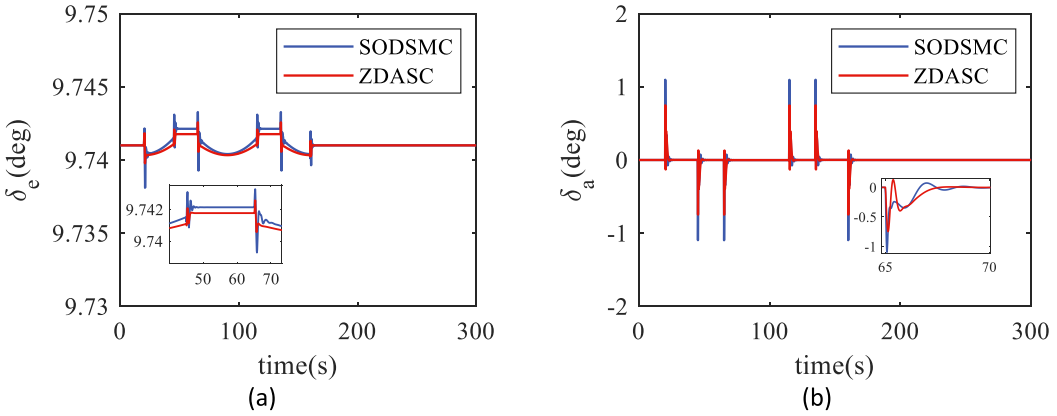

FIGURE 3. Responses of control inputs: (a) Elevator deflection δ_e, (b) Aileron deflection δ_a.

Then the output precise tracking is achieved while the zero dynamics are stable. □

Remark 2: The dynamic sliding mode control method in [23] will cause a fixed functional relationship between the equilibrium points of two internal dynamics, which prevents the precise outputs tracking [35]. In Theorem 2, the proposed ZDASC method does not rely on the ideal internal dynamics, and the internal states can adaptively stabilize under different operating conditions.

Remark 3: The $\boldsymbol{Q} \in \mathbb{R}^{5\times5}$ in Theorem 2 is a matrix with the parameters to be designed. In order to ensure that $\boldsymbol{Q}$ always satisfies the Hurwitz condition under uncertain parameters and states, intelligent optimization algorithms and other means can be used to keep the matrix eigenvalues far away from the imaginary axis. Then, the ZDASC will ensure system robustness while achieving precise tracking.

TABLE 1. RLV parameters.

Velocity($\mathrm{ft}\times\mathrm{s}^{-1}$)	$V_0 = 17192$
Mass(slug)	$m_0 = 68.5$
Gravitational acceleration($\mathrm{ft}\times\mathrm{s}^{-2}$)	$g_0 = 32.2$
Moments of inertia($\mathrm{slug}\times\mathrm{ft}^2$)	$I_x = 203.4$, $I_y = 1356$, $I_z = 1627$, $I_{xz} = 27.1$
Trim conditions(rad)	$\alpha_T = 0.66$, $\delta_{eT} = 0.17$

TABLE 2. Aerodynamic parameters.

$L'_\beta = -25.1$	$L'_{\delta_a} = -10.6$	$L_\alpha = 1200$	$Y_\beta = 2.5$
$N'_\beta = -1.53$	$N'_{\delta_a} = 0.53$	$M'_{\delta_e} = 15.1$	$M'_\alpha = 10.0$

IV. SIMULATION AND ANALYSIS

In this section, numerical simulations are performed and the results are presented to demonstrate the effectiveness and applicability of the controller design method proposed in Section III. The RLV and aerodynamic parameters are given in Table 1 and Table 2.

First, based on Theorem 1, the nonminimum phase property of the RLV attitude control system is analyzed. Substitute

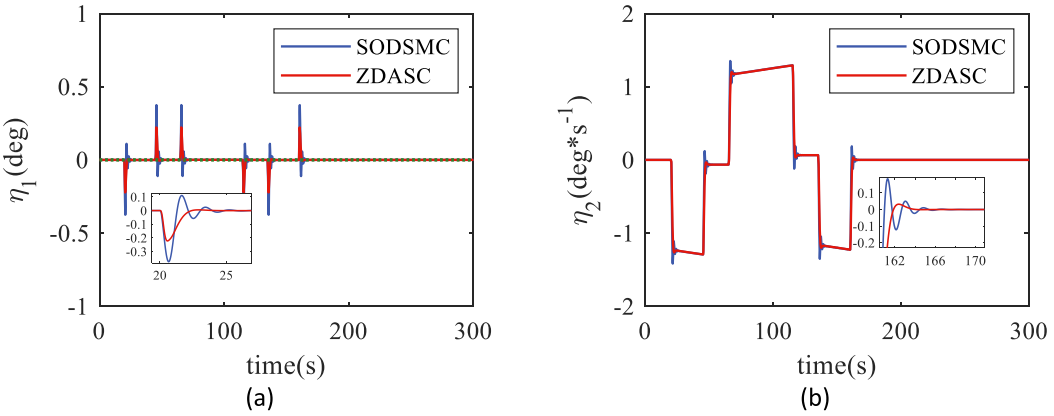

FIGURE 4. Responses of internal dynamics: (a) Curve of η_1, (b) Curve of η_2.

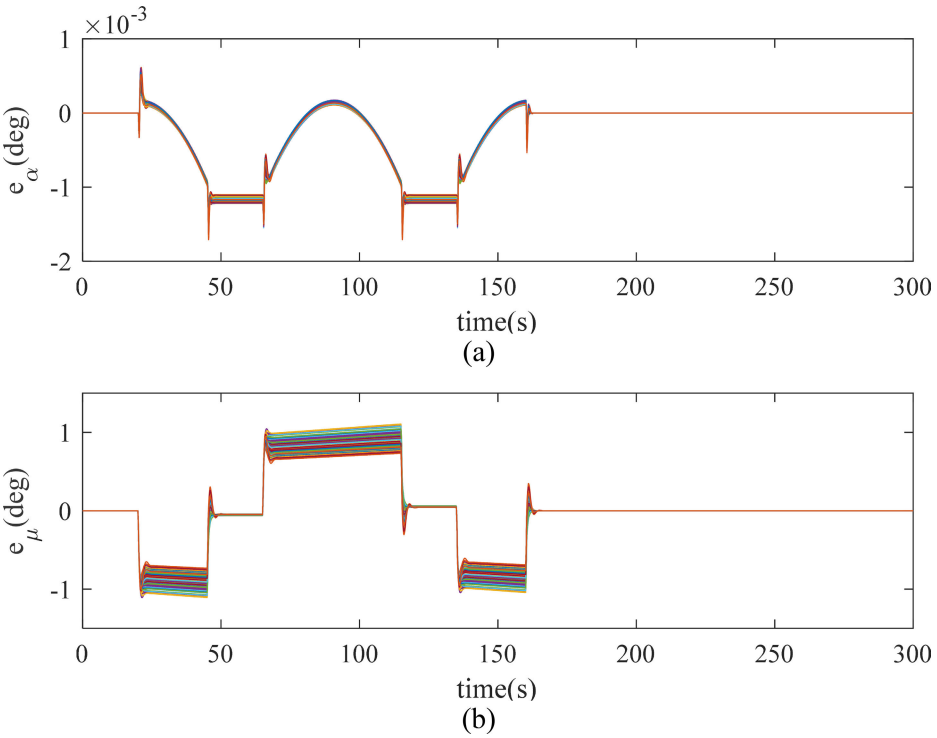

FIGURE 5. Monte carlo simulation results: (a)Angle of attack α, (b) Bank angle μ.

parameters into (10), we get

$$\cos 0.66 * 0.53 * \left(\frac{-25.1}{-10.6} - \frac{-1.53}{0.53}\right) = 2.2001 > 0 \quad (44)$$

It is revealed that the RLV attitude control system in this paper is a nonminimum phase system.

A. PERFORMANCE COMPARISON

Choosing the output commands: Keep $\alpha_c = \alpha_T = 0.66$rad(i.e. 37.818°), and μ_c changes by one cycle within the permissible ranges $[-25°, 25°]$. The control input constraints are assumed to be $\delta_e \in [0°, 50°]$ and $\delta_a \in [-25°, 25°]$ [26]. The rudders deflection rates are limited to $\left|\dot{\delta}_e\right|, \left|\dot{\delta}_a\right| < 150°/\text{s}$. The performance of the modified zero dynamic active suppression control (noted as ZDASC) proposed in this paper is compared to the second-order dynamic sliding mode control (noted as SODSMC) in [23], which also has a dynamic sliding mode structure.

The parameters of SODSMC are set as in [23]. According to the Theorem 2, the parameters of ZDASC in (19), (32), (33), (36) are given as $\lambda_{11}, \lambda_{21}, \lambda_{12}, \lambda_{22} = 0.1, \alpha_1, \alpha_2 = 0.5$, $c_1 = 1$, $\boldsymbol{G} = \left[100\ 4.33\ -93.66\ -100\ -63.83\right]^{\mathrm{T}}$, $\boldsymbol{F} = \left[-29.28\ 8.32\ 100\ -7.23\ -33.30\right]^{\mathrm{T}}$.

In the simulations, nonlinear functions $fal(\cdot)$ is used instead of sign functions in (19) and (36) to eliminate

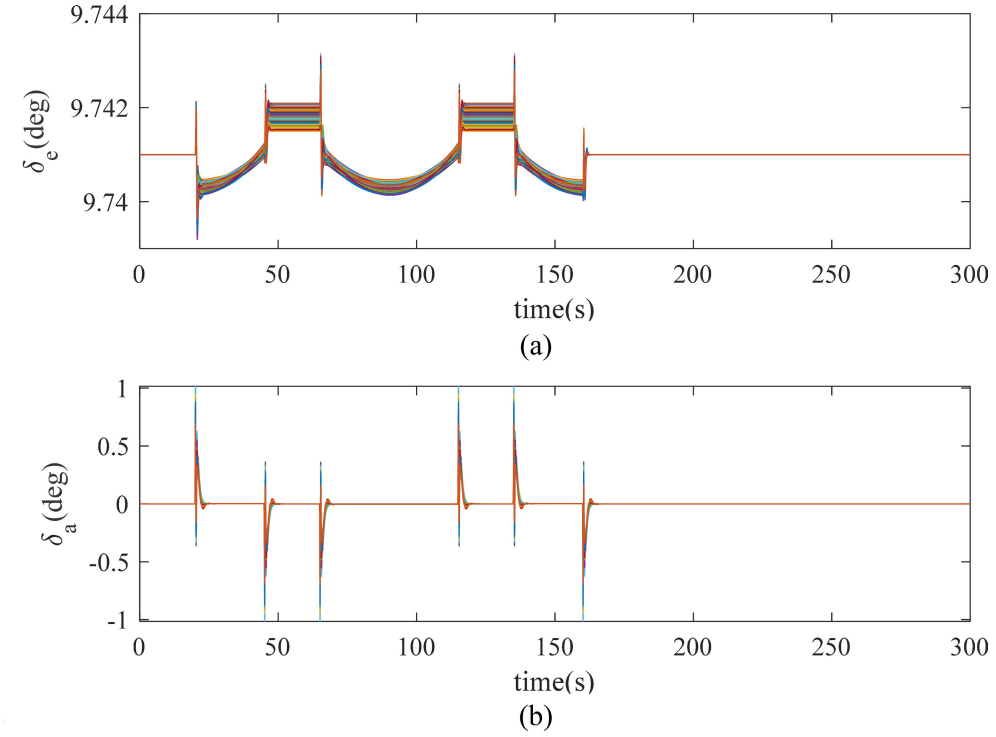

FIGURE 6. Monte carlo simulation results: (a) Elevator deflection δ_e, (b) Aileron deflection δ_a.

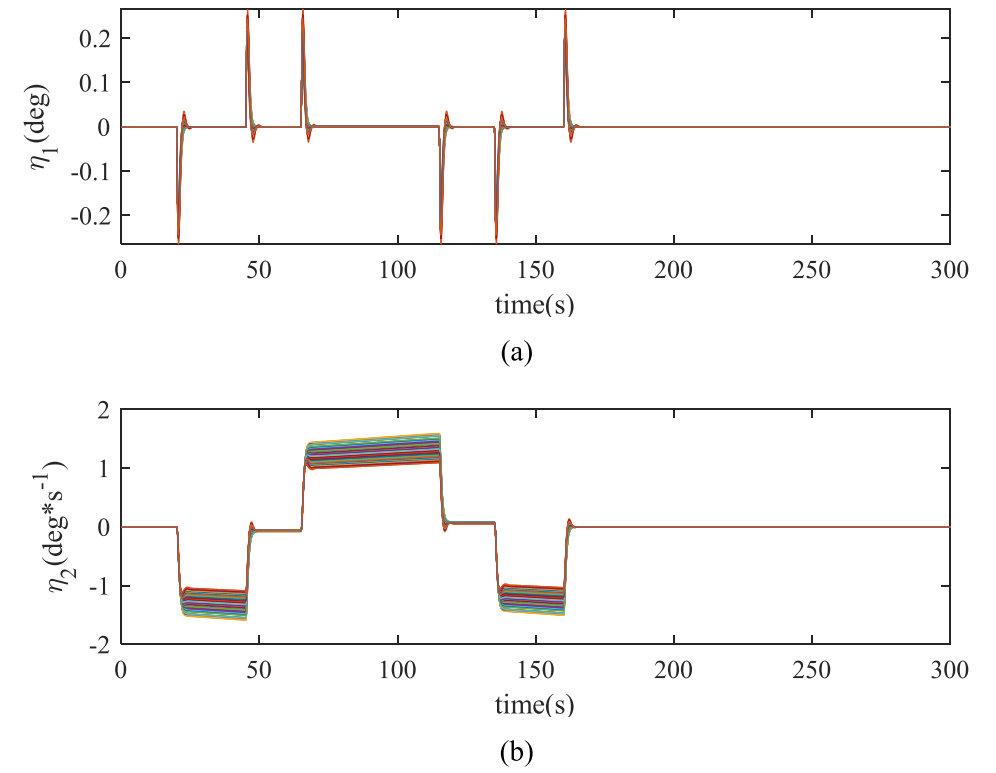

FIGURE 7. Monte carlo simulation results: (a) Internal dynamic η_1, (b) Internal dynamic η_2.

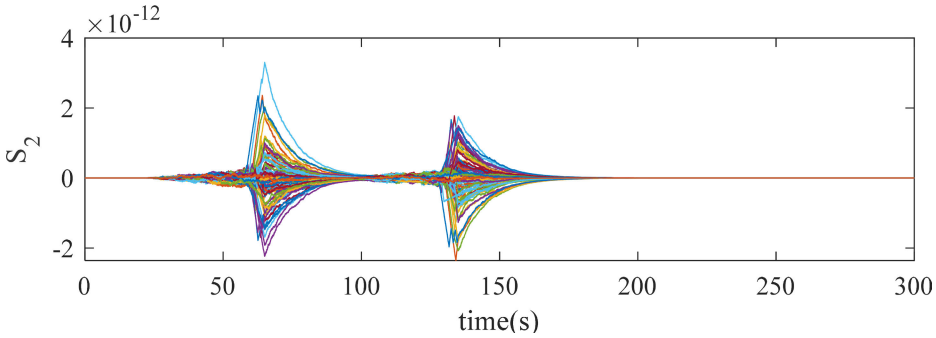

FIGURE 8. Monte carlo simulation results: S_2.

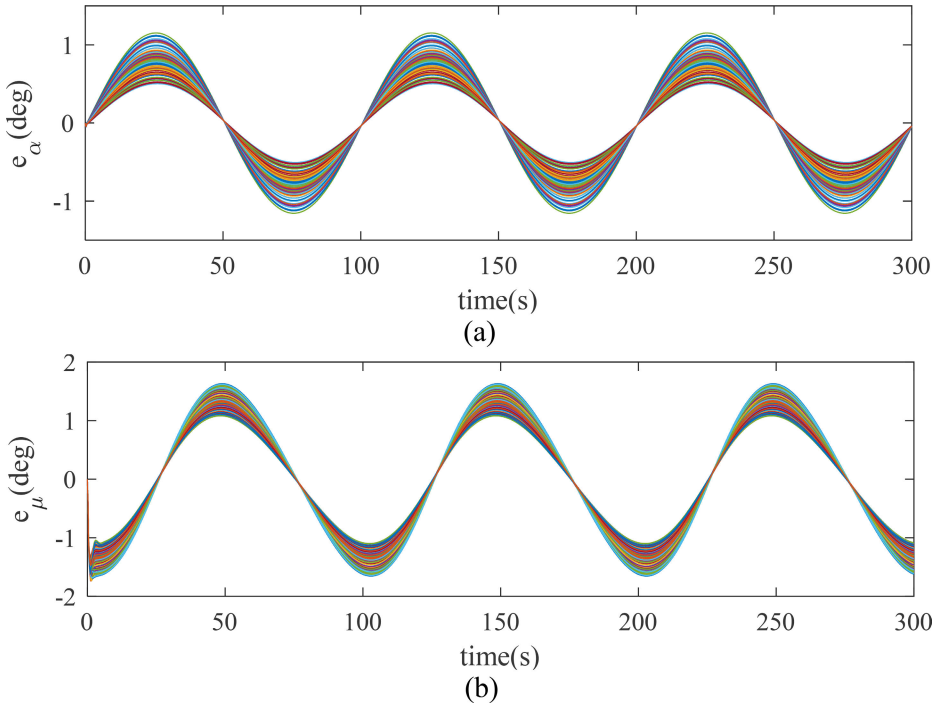

FIGURE 9. Monte carlo simulation results: (a)Angle of attack α, (b) Bank angle μ.

chattering. It is defined as

$$fal\,(e,\alpha_3,\delta) = \begin{cases} |e|^{\alpha_3}\,\mathrm{sgn}\,(e)\,, |e| > \delta \\ \dfrac{e}{\delta^{1-\alpha_3}}, |e| \le \delta \end{cases} \tag{45}$$

where e is the input variable, α_3 and δ are parameters to be determined. In this work, parameters in (45) are given as $\alpha_3 = 0.25$ and $\delta = 0.01$.

Figs. 2-4 show a comparison of the simulation results between SODSMC and ZDASC. It can be observed that the ZDASC is provided with smaller tracking error, and the outputs and inputs δ_e and δ_a obtained by ZDASC change much more smoothly. To especially, Fig. 4 shows that the internal dynamics are effectively stabilized simultaneously, and the defect caused by nonminimum phase behavior of the model is eliminated.

B. ROBUSTNESS

To verify the robustness of the ZDASC method, tracking tasks are set under parameter uncertainty conditions. Retain the commands of angle of attack and bank angle, and conduct 100 Monte Carlo simulations. Figs. 5-8 show the results of 100 Monte Carlo runs considering model uncertainties, where the aerodynamic parameter in the model are assumed to have a random deviation within $\pm 20\%$ from their nominal values. It can be observed that the two outputs tracking errors and the sideslip angle can converge to a small region around zero, and no saturation is observed for the responses of inputs δ_e and δ_a. The Monte Carlo simulations indicate that ZDASC method has good robustness against model uncertainties.

Set the attack angle and tilt angle to sine commands, with an attack angle amplitude of 5°, a bank angle amplitude of 25°, and sine period of 100 seconds, while

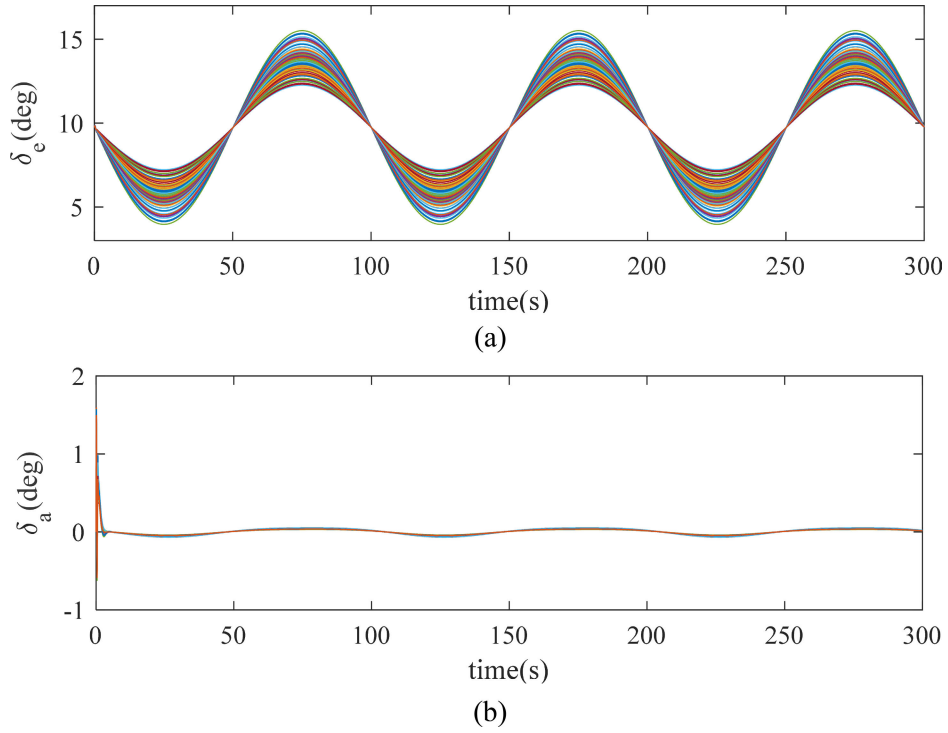

FIGURE 10. Monte carlo simulation results: (a) Elevator deflection δ_e, (b) Aileron deflection δ_a.

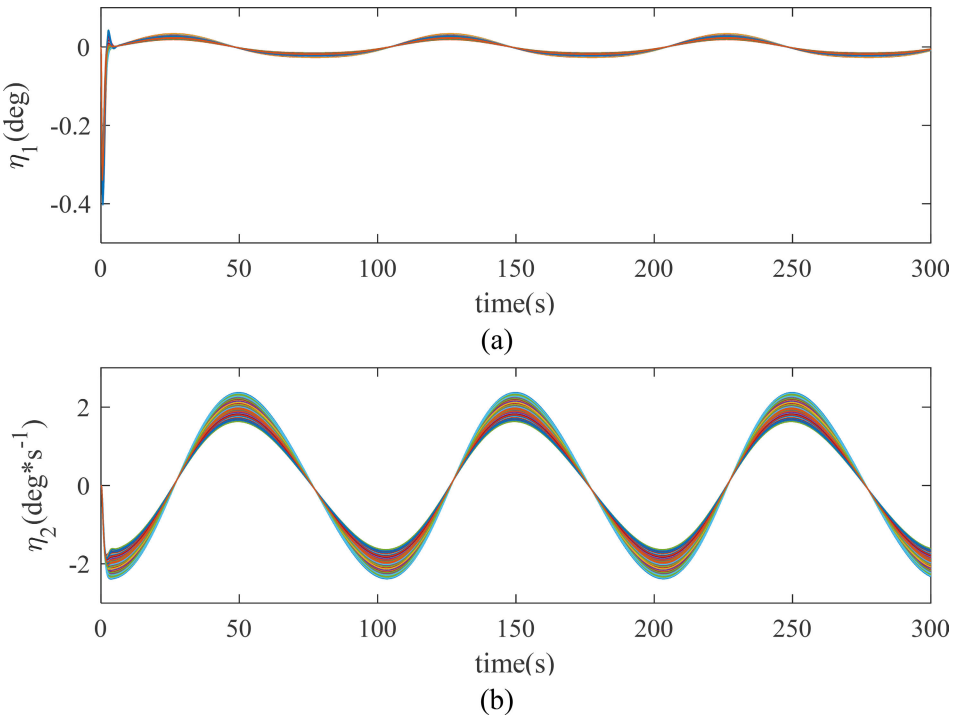

FIGURE 11. Monte carlo simulation results: (a) Internal dynamic η_1, (b) Internal dynamic η_2.

still maintaining ±20% parameter uncertainty, and conduct 100 Monte Carlo simulations. Figs. 9-12 show the results of 100 Monte Carlo runs of sine commands considering model uncertainties.

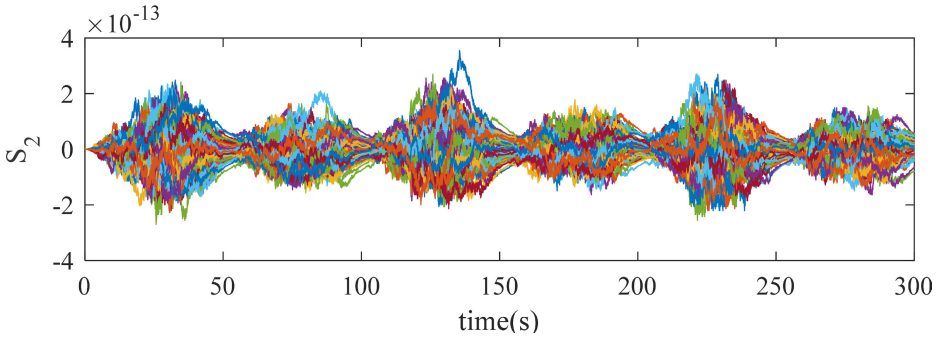

FIGURE 12. Monte carlo simulation results: S_2.

It can be observed that the two outputs tracking errors and the sideslip angle can converge to a small region around origin, and no saturation is observed for the responses of inputs δ_e and δ_a. The Monte Carlo simulations indicate that ZDASC method presents good robustness against model uncertainties.

V. CONCLUSION

A zero dynamic active suppression control (ZDASC) scheme is developed for an underactuated nonminimum phase RLV system. First, the RLV system is converted to B-I standard form, based on which a criterion of nonminimum phase property is given by the stability analysis of internal dynamics. A B-I-based ZDASC method is proposed, achieving asymptotic tracking of outputs while stabilizing internal dynamics.

The salient features of the proposed approach are twofold. One is presenting a computable criterion for the nonminimum phase property of RLVs based on its B-I standard model, by which we can effectively determine the nonminimum phase property based on aerodynamic parameters of the RLV model. The other is transforming the output tracking problem into stabilization problem of an augmented system consisting of internal dynamics and dynamic compensator. ZDASC achieves output accurate tracking without solving the ideal internal dynamics, which reduces the computational complexity and enhances system robustness. In particular, the overall approach shown here provides a practical solution to achieving RLV reentry attitude tracking control under realistic conditions. It confirms the advantages of the proposed method by contrast simulations and Monte Carlo simulations conducted in this work. The proposed control architecture may also be applied to other underactuated nonminimum systems.

REFERENCES

[1] W. Li, J. Zhao, S. Su, R. Mo, and Y. Lin, "Adaptive output feedback attitude control for reusable launch vehicle with input constraints and actuator faults," *Aerosp. Sci. Technol.*, vol. 142, Nov. 2023, Art. no. 108616.

[2] B.-U. Jo and J. Ahn, "Optimal staging of reusable launch vehicles for minimum life cycle cost," *Aerosp. Sci. Technol.*, vol. 127, Aug. 2022, Art. no. 107703.

[3] F. Wang, Q. Zong, and B. Tian, "Adaptive backstepping finite time attitude control of reentry RLV with input constraint," *Math. Problems Eng.*, vol. 2014, pp. 1–19, Jan. 2014.

[4] M. Li and J. Hu, "An approach and landing guidance design for reusable launch vehicle based on adaptive predictor–corrector technique," *Aerosp. Sci. Technol.*, vol. 75, pp. 13–23, Apr. 2018.

[5] R. Sarkar, S. M. Amrr, J. K. Bhutto, A. S. Saidi, A. Algethami, and A. Banerjee, "Finite time fractional order ISMC with time delay estimation for re-entry phase of RLV with enhanced chattering suppression," *Acta Astronautica*, vol. 202, pp. 130–138, Jan. 2023.

[6] A. Scottedward Hodel and C. E. Hall, "Variable-structure PID control to prevent integrator windup," *IEEE Trans. Ind. Electron.*, vol. 48, no. 2, pp. 442–451, Apr. 2001.

[7] Z. Xu and S. Tang, "RLV (Reusable launch vehicle) reentry nonlinear controller design," in *Proc. IEEE-CMCE*, Changchun, China, 2010, pp. 380–383.

[8] S. E. Skariya, B. Sebastian, and M. N. Namboodiripad, "Integrated optimal control of reusable launch vehicle and actuation system using linear quadratic regulator," *IFAC Proc. Volumes*, vol. 47, no. 1, pp. 840–846, 2014.

[9] A. Li, L. Yang, and J. Zhang, "LQR and fuzzy gain-scheduling based attitude controller for RLV within large operating envelope," in *Proc. IEEE-ICCSSE*, Yantai, China, Mar. 2014, pp. 51–56.

[10] P. V. Gauri and R. Hari Kumar, "A comparison of optimal LQR controller and robust H∞ controller for RLV," in *Proc. 2nd Int. Conf. Intell. Comput. Control Syst. (ICICCS)*, Jun. 2018, pp. 1055–1060.

[11] J. Georgie and J. Valasek, "Evaluation of longitudinal desired dynamics for dynamic-inversion controlled generic reentry vehicles," *J. Guid., Control, Dyn.*, vol. 26, no. 5, pp. 811–819, Sep. 2003.

[12] B. Tian, Z. Li, X. Zhang, and Q. Zong, "Adaptive prescribed performance attitude control for RLV with mismatched disturbance," *Aerosp. Sci. Technol.*, vol. 117, Oct. 2021, Art. no. 106918.

[13] J. Sun, J. Yi, Z. Pu, and X. Tan, "Fixed-time sliding mode disturbance observer-based nonsmooth backstepping control for hypersonic vehicles," *IEEE Trans. Syst., Man, Cybern., Syst.*, vol. 50, no. 11, pp. 4377–4386, Nov. 2020.

[14] Q. Lam, P. Krishnamurthy, and F. Khorrami, "Enhancing flight control system performance using SDRE based controller as an augmentation layer," in *Proc. AIAA Guid., Navigat., Control Conf.*, Chicago, IL, USA, Aug. 2009, pp. 2009–6171.

[15] Q. Lam and M. Xin, "Robustness evaluation of theta-D technique for spacecraft attitude control subject to reaction wheel failures," in *Proc. AIAA Guid., Navigat., Control Conf.*, Toronto, ON, Canada, Aug. 2010, pp. 2010–8302.

[16] X. Liang, B. Xu, R. Hong, and M. Sang, "Quaternion observer-based sliding mode attitude fault-tolerant control for the reusable launch vehicle during reentry stage," *Aerosp. Sci. Technol.*, vol. 129, Oct. 2022, Art. no. 107855.

[17] B. Li, Q. Hu, and Y. Yang, "Continuous finite-time extended state observer based fault tolerant control for attitude stabilization," *Aerosp. Sci. Technol.*, vol. 84, pp. 204–213, Jan. 2019.

[18] C. Xiu and P. Guo, "Global terminal sliding mode control with the quick reaching law and its application," *IEEE Access*, vol. 6, pp. 49793–49800, 2018.

[19] Z. Yang, D. Zhang, X. Sun, and X. Ye, "Adaptive exponential sliding mode control for a bearingless induction motor based on a disturbance observer," *IEEE Access*, vol. 6, pp. 35425–35434, 2018.

[20] J. Liu, J. Shan, J. Wang, and J. Rong, "Incremental sliding-mode control and allocation for morphing-wing aircraft fast manoeuvring," *Aerosp. Sci. Technol.*, vol. 131, Dec. 2022, Art. no. 107959.
[21] Q. Sun, L. Yu, Y. Zheng, J. Tao, H. Sun, M. Sun, M. Dehmer, and Z. Chen, "Trajectory tracking control of powered parafoil system based on sliding mode control in a complex environment," *Aerosp. Sci. Technol.*, vol. 122, Mar. 2022, Art. no. 107406.
[22] W. R. van Soest, Q. P. Chu, and J. A. Mulder, "Combined feedback linearization and constrained model predictive control for entry flight," *J. Guid., Control, Dyn.*, vol. 29, no. 2, pp. 427–434, Mar. 2006.
[23] Z. Wang, W. Bao, and H. Li, "Second-order dynamic sliding-mode control for nonminimum phase underactuated hypersonic vehicles," *IEEE Trans. Ind. Electron.*, vol. 64, no. 4, pp. 3105–3112, Apr. 2017.
[24] E. M. Wallner and K. H. Well, "Attitude control of a reentry vehicle with internal dynamics," *J. Guid., Control, Dyn.*, vol. 26, no. 6, pp. 846–854, Nov. 2003.
[25] L. Ye, Q. Zong, and B. Tian, "Output tracking of uncertain nonminimum phase systems by experience replay," *IEEE Trans. Syst., Man, Cybern., Syst.*, vol. 51, no. 5, pp. 3159–3167, May 2021.
[26] L. Ye, B. Tian, H. Liu, Q. Zong, B. Liang, and B. Yuan, "Anti-windup robust backstepping control for an underactuated reusable launch vehicle," *IEEE Trans. Syst., Man, Cybern., Syst.*, vol. 52, no. 3, pp. 1492–1502, Mar. 2022.
[27] Z. Wang, H. F. Li, and W. M. Bao, "Body-flap attitude control method for lifting re-entry vehicle," *J. Beijing Univ. Aeronaut. Astronaut.*, vol. 42, pp. 532–541, Mar. 2016.
[28] Z. Guo, J. Guo, and J. Zhou, "Adaptive attitude tracking control for hypersonic reentry vehicles via sliding mode-based coupling effect-triggered approach," *Aerosp. Sci. Technol.*, vol. 78, pp. 228–240, Jul. 2018.
[29] A. Isidori and C. Byrnes, "Output regulation of nonlinear systems," *IEEE Trans. Autom. Control*, vol. 35, no. 2, pp. 131–140, Feb. 1990.
[30] J. Huang, *Nonlinear Output Regulation: Theory and Application*. Philadelphia, PA, USA: SIAM, 2004.
[31] I. A. Shkolnikov and Y. B. Shtessel, "Tracking controller design for a class of nonminimum-phase systems via the method of system center," *IEEE Trans. Autom. Control*, vol. 46, no. 10, pp. 1639–1643, Oct. 2001.
[32] I. A. Shkolnikov and Y. B. Shtessel, "Tracking in a class of nonminimum-phase systems with nonlinear internal dynamics via sliding mode control using method of system center," *Automatica*, vol. 38, no. 5, pp. 837–842, May 2002.
[33] S. Devasia, D. Chen, and B. Paden, "Nonlinear inversion-based output tracking," *IEEE Trans. Autom. Control*, vol. 41, no. 7, pp. 930–942, Jul. 1996.
[34] Q. Zou and S. Devasia, "Precision preview-based stable-inversion for nonlinear nonminimum-phase systems: The VTOL example," *Automatica*, vol. 43, no. 1, pp. 117–127, Jan. 2007.
[35] Y. Wang, T. Chao, S. Wang, and M. Yang, "Byrnes-isidori-based dynamic sliding-mode control for nonminimum phase hypersonic vehicles," *Aerosp. Sci. Technol.*, vol. 95, Dec. 2019, Art. no. 105478.
[36] H. Li, *Hypersonic Aircraft Guidance and Control Technology*, vol. 1. Beijing, China: Astronautic Publ. House, Dec. 2012, ch. 2, pp. 77–83.
[37] S. A. Snell, D. F. Enns, and W. L. Garrard, "Nonlinear inversion flight control for a supermaneuverable aircraft," *J. Guid., Control, Dyn.*, vol. 15, no. 4, pp. 976–984, Jul. 1992.
[38] M. P. Aghababa, S. Khanmohammadi, and G. Alizadeh, "Finite-time synchronization of two different chaotic systems with unknown parameters via sliding mode technique," *Appl. Math. Model.*, vol. 35, no. 6, pp. 3080–3091, Jun. 2011.

YUXIAO WANG received the B.S., M.S., and Ph.D. degrees from Harbin Institute of Technology, China, in 2012, 2014, and 2019, respectively. He is currently a Lecturer with the College of Electronic Information and Automation, Civil Aviation University of China. His research interests include spacecraft guidance and control, modeling, and optimization of complex systems.

YUYU ZHAO received the B.S., M.S., and Ph.D. degrees from Harbin Institute of Technology, China, in 2012, 2014, and 2019, respectively. She is currently a Lecturer with the College of Electronic Information and Automation, Civil Aviation University of China. Her research interests include spacecraft attitude control and inertial instruments.

GAOWEI ZHANG received the B.S. and Ph.D. degrees from Hebei University of Technology, Tianjin, China, in 2014 and 2021, respectively. He is currently a Lecturer with the College of Electronic Information and Automation, Civil Aviation University of China. His research interests include nonlinear control theory, sliding mode control, and wearable exoskeleton.